

Robust model selection between population growth and multiple merger coalescents

Jere Koskela
j.koskela@warwick.ac.uk
Department of Statistics
University of Warwick
Coventry, CV4 7AL
United Kingdom

Maite Wilke Berenguer
wilkeber@math.tu-berlin.de
Institut für Mathematik
Technische Universität Berlin
Straße des 17. Juni 136, 10623 Berlin,
Germany

October 23, 2019

Abstract

We study the effect of biological confounders on the model selection problem between Kingman coalescents with population growth, and Ξ -coalescents involving simultaneous multiple mergers. We use a low dimensional, computationally tractable summary statistic, dubbed the *singleton-tail statistic*, to carry out approximate likelihood ratio tests between these models. The singleton-tail statistic has been shown to distinguish between the two classes with high power in the simple setting of neutrally evolving, panmictic populations without recombination. We extend this work by showing that cryptic recombination and selection do not diminish the power of the test, but that misspecifying population structure does. Furthermore, we demonstrate that the singleton-tail statistic can also solve the more challenging model selection problem between multiple mergers due to selective sweeps, and multiple mergers due to high fecundity with moderate power of up to 60%.

1 Introduction

The Kingman coalescent [Kingman, 1982a,b,c, Hudson, 1983a,b, Tajima, 1983] models random ancestral relations among large populations as random, binary trees, and is an important tool for predicting genetic diversity. A central assumption of the Kingman coalescent is that the variance of family sizes is small, so that the large population always consists of many relatively small families. Violations of this assumption lead to more general Λ -coalescents, which allow more than two lineages to merge to a common ancestor simultaneously [Sagitov, 1999, Pitman, 1999, Donnelly and Kurtz, 1999a]. Such *multiple merger* events correspond to very large families, which call for models with family size distributions that have infinite variance.

There is growing evidence that Λ -coalescents are an appropriate model for organisms with high fecundity coupled with a skewed offspring distribution [Beckenbach, 1994, Árnason, 2004, Eldon and Wakeley, 2006, Sargsyan and Wakeley, 2008, Hedgecock and Pudovkin, 2011, Birkner et al., 2011, Steinrücken et al., 2013, Tellier and Lemaire, 2014]. Consequently, development of statistical techniques for distinguishing between Kingman-type coalescents and coalescents with multiple mergers has also been an active area of research [Eldon et al., 2015, Koskela, 2018]. In particular, attention has focused on distinguishing Λ -coalescents from Kingman coalescents with population growth, because both classes of models predict an excess of singleton mutations (mutations only carried by one individual in a sample of DNA sequences) relative to the standard Kingman coalescent when the infinitely many sites model of mutation [Watterson, 1975] is assumed.

Koskela [2018] introduced a simple, two-dimensional summary statistic, referred to here as the *singleton-tail* statistic, which distinguishes between these model classes with high power even from a modest data set consisting of 500 samples from bi-parental, diploid organisms sequenced at around 10 unlinked chromosomes. It was also demonstrated that the correct model could be selected with high power without knowing the mutation rate, provided it is not very small (see also [Eldon et al., 2015, Supporting Information 12]). In this paper we investigate the impact of other confounders on the prospect of discriminating between these models based on the singleton-tail statistic, again in the bi-parental, diploid setting. In particular, we will focus on each of

1. weak natural selection modelled by the Ancestral Selection Graph [Krone and Neuhauser, 1997, Neuhauser and Krone, 1997, Donnelly and Kurtz, 1999b],
2. recombination modelled by the Ancestral Recombination Graph [Hudson, 1983a, Griffiths and Marjoram, 1997, Donnelly and Kurtz, 1999b, Birkner et al., 2013],
3. population structure modelled by the structured coalescent [Herbots, 1997, Eldon, 2009],

and show that the presence or absence of the first two does not affect the statistical power of the hypothesis test developed in [Koskela, 2018], while population structure is a significant confounder that must be correctly incorporated into the inference procedure. Note that in the diploid, bi-parental setting there are four parental chromosomes involved in each merger, allowing for up to four separate merger events at any one time. Hence the models considered in this paper are actually Ξ -coalescents [Schweinsberg, 2000, Möhle and Sagitov, 2001] which allow simultaneous multiple mergers, despite the fact that the population is assumed to reproduce in a fashion consistent with the more restrictive Λ -coalescent class permitting only one multiple merger at any given time.

In addition, we use the singleton-tail statistic to distinguish diploid Ξ -coalescents arising from high fecundity reproduction from diploid Ξ -coalescents arising from selective sweeps [Durrett and Schweinsberg, 2005]. This problem is more challenging than a null hypothesis consisting of Kingman coalescents with population growth, because the marginal coalescent process at each chromosome can be identical under the two hypotheses. However, high fecundity reproduction results in positively correlated coalescence times between unlinked chromosomes, while under the selective sweep model the coalescent processes at unlinked chromosomes are independent. The singleton-tail statistic is able to detect the positive correlation as increased sampling variance, which results in tests with moderate statistical power of up to 60% even in this challenging setting.

The rest of the paper is organised as follows. In Section 2 we recall the singleton-tail statistic of [Koskela, 2018] as well as the associated hypothesis test for model selection. Section 3 presents a unified, diploid coalescent model incorporating high fecundity reproduction and population growth, as well as the three confounders of weak selection, crossover recombination, and discrete spatial structure. Models with only population growth or high fecundity reproduction, as well as any desired subset of confounders, can be recovered as special cases. Section 4 provides simulation studies on the effect of each of the confounders on the sampling distribution of the singleton-tail statistic, as well as on the power of the hypothesis test introduced in Section 2. In Section 5 we apply the singleton-tail statistic to the much harder problem of distinguishing multiple mergers due to high fecundity reproduction acting globally on the genome, from multiple mergers caused by selective sweeps acting locally on the genome. Section 6 concludes with a discussion.

2 The singleton-tail statistic

Suppose a sample of $n \in \mathbb{N}$ DNA sequences at a single chromosome is available, and that derived mutations can be distinguished from ancestral states. Let $[n] := \{1, \dots, n\}$, and let $\xi_i^{(n)}$ be the number of sites at which a mutant allele appears $i \in [n-1]$ times. Then

$$\boldsymbol{\xi}^{(n)} := \left(\xi_1^{(n)}, \dots, \xi_{n-1}^{(n)} \right)$$

is the *unfolded site-frequency spectrum* (SFS). If mutant and ancestral types cannot be distinguished, the *folded* spectrum $\boldsymbol{\eta}^{(n)} := (\eta_1^{(n)}, \dots, \eta_{\lfloor n/2 \rfloor}^{(n)})$ [Fu, 1995] is used instead, where

$$\eta_i^{(n)} := \frac{\xi_i^{(n)} + \xi_{n-i}^{(n)}}{1 + \delta_{i,n-i}}, \quad 1 \leq i \leq \lfloor n/2 \rfloor,$$

and $\delta_{i,j} = 1$ if $i = j$, and is zero otherwise. Let $\boldsymbol{\zeta}^{(n)} := (\zeta_1^{(n)}, \dots, \zeta_{n-1}^{(n)})$ be the normalised unfolded SFS, whose entries are given by $\zeta_i^{(n)} := \xi_i^{(n)} / |\boldsymbol{\xi}^{(n)}|$, where $|\boldsymbol{\xi}^{(n)}| := \xi_1^{(n)} + \dots + \xi_{n-1}^{(n)}$ is the total number of segregating sites, and with the convention that $\boldsymbol{\zeta}^{(n)} = \mathbf{0}$ if there are no segregating sites.

Now define the *lumped tail* of the SFS as

$$\bar{\zeta}_k^{(n)} := \sum_{j=k}^{n-1} \zeta_j^{(n)}, \quad 3 \leq k \leq n-1$$

and consider the summary statistic $(\zeta_1^{(n)}, \bar{\zeta}_k^{(n)})$ for some fixed k . Multi-chromosome data is incorporated by averaging: if L unlinked chromosomes are available, then the singleton-tail statistic is

$$(\zeta_{1,L}^{(n)}, \bar{\zeta}_{k,L}^{(n)}) := \frac{1}{L} \sum_{j=1}^L (\zeta_1^{(n)}(j), \bar{\zeta}_k^{(n)}(j)),$$

where $(\zeta_1^{(n)}(j), \bar{\zeta}_k^{(n)}(j))$ denote the singleton class and lumped tail computed from the j^{th} chromosome.

For two classes of models Θ_0 and Θ_1 , the likelihood ratio test statistic is

$$\frac{\sup_{\Pi \in \Theta_1} P^{\Pi}(\zeta_{1,L}^{(n)}, \bar{\zeta}_{k,L}^{(n)})}{\sup_{\Pi \in \Theta_0} P^{\Pi}(\zeta_{1,L}^{(n)}, \bar{\zeta}_{k,L}^{(n)})},$$

where P^{Π} denotes the sampling distribution of the singleton-tail statistic under coalescent process Π . A corresponding hypothesis test of size ω given an observed value of the singleton-tail statistic is

$$\Phi(\zeta_{1,L}^{(n)}, \bar{\zeta}_{k,L}^{(n)}) = \begin{cases} 0 & \text{if } \frac{\sup_{\Pi \in \Theta_1} P^{\Pi}(\zeta_{1,L}^{(n)}, \bar{\zeta}_{k,L}^{(n)})}{\sup_{\Pi \in \Theta_0} P^{\Pi}(\zeta_{1,L}^{(n)}, \bar{\zeta}_{k,L}^{(n)})} \leq q_{\omega} \\ 1 & \text{if } \frac{\sup_{\Pi \in \Theta_1} P^{\Pi}(\zeta_{1,L}^{(n)}, \bar{\zeta}_{k,L}^{(n)})}{\sup_{\Pi \in \Theta_0} P^{\Pi}(\zeta_{1,L}^{(n)}, \bar{\zeta}_{k,L}^{(n)})} > q_{\omega} \end{cases}, \quad (1)$$

where $\Phi(\zeta_{1,L}^{(n)}, \bar{\zeta}_{k,L}^{(n)}) = 1$ corresponds to rejecting the null hypothesis Θ_0 , and q_{ω} is the quantile

$$\sup_{\Pi \in \Theta_0} \mathbb{P}^{\Pi} \left(\frac{\sup_{\Pi \in \Theta_1} P^{\Pi}(\zeta_{1,L}^{(n)}, \bar{\zeta}_{k,L}^{(n)})}{\sup_{\Pi \in \Theta_0} P^{\Pi}(\zeta_{1,L}^{(n)}, \bar{\zeta}_{k,L}^{(n)})} \geq q_{\omega} \right) \leq \omega.$$

The sampling distribution P^Π and the quantile q_ω are both intractable, but can easily be approximated by simulation due to the low dimensionality of the singleton-tail statistic to obtain an implementable hypothesis test with approximate size ω Koskela [2018]. In particular, Koskela [2018] considers the hypotheses

$$\begin{aligned}\Theta_0 &:= \{\text{Kingman coalescent with exponential or algebraic growth at rates } \gamma \in \{0, 0.1, \\ &\quad 0.2, \dots, 0.9, 1, 1.5, 2, 2.5, 3, 3.5, 4, 5, 6, \dots, 19, 20, 25, 30, 35, 40, 50, 60, \dots, 990, 1000\}\}, \\ \Theta_1 &:= \{\text{Beta}(2 - \alpha, \alpha)\text{-}\Xi\text{-coalescents with } \alpha \in \{1, 1.025, \dots, 1.975, 2\}\},\end{aligned}\tag{2}$$

which will also be the focus of this paper. In brief, data is simulated under both Θ_0 and Θ_1 , and kernel density estimates (KDEs) \hat{P}^Π of the intractable sampling distributions P^Π are obtained for $\Pi \in \Theta_0$ and $\Pi \in \Theta_1$. These KDEs, along with more simulated data, can be used to accurately approximate the intractable quantile q_ω , yielding an implementable hypothesis test.

Producing simulated data in order to approximate the test based on (1) requires specification of the cutoff k from which the tail of the singleton-tail statistic is lumped, as well as of the mutation rate θ . However, sensitivity analyses conducted in Koskela [2018] showed that the test was highly insensitive to the choice of k provided $k \gtrsim 6$, as well as of misspecification of the mutation rate. Hence, in practice it suffices to use the generalised Watterson estimator,

$$\hat{\theta} = |\xi^{(n)}|/\mathbb{E}^\Pi[T^{(n)}],$$

where $\mathbb{E}^\Pi[T^{(n)}]$ denotes the expected tree height from n leaves under coalescent mechanism Π . In contrast, increasing the number of unlinked chromosomes always improved the performance of hypothesis tests.

3 An umbrella model

In this section we describe a general class of models incorporating diploidy, bi-parental, high fecundity reproduction, population growth, weak natural selection, population structure in a discrete geography, and crossover recombination. Models with any subset of the above forces can then be recovered as special cases.

Consider a geography of D demes, with the historical population size on deme $i \in \{1, \dots, D\}$ at time $t \geq 0$ generations ago being given by

$$M_N^{(i)}(t) := 2 \left\lfloor Nd_i \left(1 + \frac{\gamma_i}{2\lfloor Nd_i \rfloor}\right)^{-t} \right\rfloor,\tag{3}$$

for $N \in \mathbb{N}$, $\gamma_i \geq 0$, and $d_i > 0$ with $d_1 + \dots + d_D = 1$. Each individual is diploid, and carries $L \in \mathbb{N}$ pairs of unlinked chromosomes. Each chromosome carries one of $K \in \mathbb{N}$ alleles, which we identify with $\{1, \dots, K\}$, and which are acted upon by natural selection. In addition to this selectively active allele, each chromosome is identified with the unit interval $[0, 1]$, on which neutral mutations and crossover recombination take place. For definiteness, we assume that the selectively active allele is determined by a non-recombining segment of material attached to the left end of the neutral interval.

The population evolves in discrete time with non-overlapping generations. At each time step t , the individuals on all demes reproduce, with those on deme i forming $M_N^{(i)}(t)/2$ pairs uniformly at random. Each pair is assigned a fitness

$$s_N((h_1^{(i,j_1)}, \dots, h_L^{(i,j_1)}; h_{L+1}^{(i,j_1)}, \dots, h_{2L}^{(i,j_1)}), (h_1^{(i,j_2)}, \dots, h_L^{(i,j_2)}; h_{L+1}^{(i,j_2)}, \dots, h_{2L}^{(i,j_2)})),$$

where $h_l^{(i,j)}$ denotes the allele on chromosome l of parent j on deme i . The fitness function s_N is assumed to satisfy the symmetry condition

$$s_N(h^{(i,j_1)}, h^{(i,j_2)}) = s_N(h^{(i,j_2)}, h^{(i,j_1)}),$$

where $h^{(i,j)} = (h_1^{(i,j)}, \dots, h_L^{(i,j)}; h_{L+1}^{(i,j)}, \dots, h_{2L}^{(i,j)})$ denotes the vector of alleles on the $2L$ chromosomes of parent j on deme i .

Each pair now produces both neutral and selective offspring to form the next generation. We fix some arbitrary ordering of the pairs of parents on each deme, and denote the number of neutral (resp. selective) offspring produced by pair j on deme i by $\nu_j^{(i)}$ (resp. $\beta_j^{(i)}$). The vectors of neutral offspring $\left(\nu_1^{(i)}, \dots, \nu_{M_N^{(i)}(t)/2}^{(i)}\right)$ are assumed to be exchangeable, independent across demes and time steps, and identically distributed across time steps, while the vectors of selective offspring $\left(\beta_1^{(i)}, \dots, \beta_{M_N^{(i)}(t)/2}^{(i)}\right)$ are independent across demes and time steps. In addition, both vectors on each island are assumed to satisfy the almost sure constraint

$$\sum_{j=1}^{M_N^{(i)}(t)/2} \nu_j^{(i)} + \beta_j^{(i)} \equiv M_N^{(i)}(t-1).$$

Each offspring now inherits one chromosome from each of its parents. Each inherited chromosome is a mosaic of the two parental chromosomes, with the number of recombination breakpoints having the geometric distribution with parameter r_N , and each break point being uniformly distributed along the chromosome. All of the geometric and uniform random variables are independent of each other, as well as the wider reproduction mechanism. Thus, the heredity of the chromosome pair becomes a mosaic of the two parents. Each chromosome inherits its allele from the parental chromosome assigned to its leftmost segment, with selective mutations happening independently at random with probability μ_N . Mutant types are drawn from a stochastic matrix M .

Finally, a deterministic fraction $m_{i_1 i_2}^{(N)}$ of the children chosen uniformly at random from deme i_1 migrate to deme i_2 , for each pair of demes. These migration fractions are assumed to satisfy

$$M_N^{(i_1)}(t) \sum_{i_2=1}^D m_{i_1 i_2}^{(N)} \equiv \sum_{i_2=1}^D M_N^{(i_2)}(t) m_{i_2 i_1}^{(N)}, \quad (4)$$

for each $t \geq 0$, so that the population sizes of the demes are unchanged by migration.

Define

$$c_N := \frac{1}{4} \sum_{i=1}^D \frac{(2 \lfloor Nd_i \rfloor)_2}{(2N)_2} \sum_{j=1}^{\lfloor Nd_i \rfloor} \frac{\mathbb{E}[(\nu_j^{(i)})_2]}{(2 \lfloor Nd_i \rfloor)_2} \sim \frac{1}{16N} \sum_{i=1}^D d_i \mathbb{E}[(\nu_1^{(i)})_2]$$

as the (asymptotic, as $N \rightarrow \infty$) probability that two chromosomes sampled uniformly at random from the whole population were born to a common family as neutral offspring in the previous generation, made the same choice from two available parents, and also the same choice of chromosome within that parent. In other words, c_N is the asymptotic probability of two chromosomes sampled at time 0 merging to a common ancestor in one generation.

We make the following assumptions as $N \rightarrow \infty$:

$$\mathbb{E}[(\nu_1^{(i)})_2] \rightarrow \mathbb{E}[(\nu_1)_2] \text{ for every } i \in \{1, \dots, D\}, \quad (5)$$

$$c_N \rightarrow 0, \quad (6)$$

$$\frac{\mathbb{E}[(\nu_1^{(i)})_2(\nu_2^{(i)})_2]}{4[Nd_i]^2 c_N} \rightarrow 0 \text{ for } i \in \{1, \dots, D\}, \quad (7)$$

$$\frac{2[Nd_i]}{c_N} \mathbb{P}(\nu_1^{(i)} > 2Nd_i x) \rightarrow 4 \int_x^1 \frac{\Lambda(dy)}{y^2} \text{ for } i \in \{1, \dots, D\}, \text{ and some probability measure } \Lambda \text{ on } [0, 1], \quad (8)$$

$$\frac{\mu_N}{c_N} \rightarrow \theta \in [0, \infty), \quad (9)$$

$$\frac{r_N}{c_N} \rightarrow \rho \in [0, \infty), \quad (10)$$

$$\frac{m_{i_1 i_2}^{(N)}}{c_N} \rightarrow m_{i_1 i_2} \in [0, \infty) \text{ for } i_1 \neq i_2 \in \{1, \dots, D\}, \quad (11)$$

$$\mathbb{E}[\beta_j^{(i)}] = s_N(h^{(i, j_1)}, h^{(i, j_2)}) \text{ for each } i \in \{1, \dots, D\}, \text{ when index } j \text{ corresponds to the parental pair } (j_1, j_2), \quad (12)$$

$$\frac{s_N(\cdot, \cdot)}{c_N} \rightarrow \sigma(\cdot, \cdot), \quad (13)$$

$$\min\{\sigma(\cdot, \cdot)\} = 0, \quad (14)$$

$$\max\{\sigma(\cdot, \cdot)\} =: \sigma^* < \infty, \quad (15)$$

of which (14) is a convenient normalisation and is without loss of generality.

Remark 1. It is well known that if $\Lambda = \delta_0$ in (8), then the assumption is equivalent to

$$\frac{\mathbb{E}[(\nu_1^{(i)})_3]}{4[Nd_i]^2 c_N} \rightarrow 0$$

for each $i \in \{1, \dots, D\}$. This will disallow multiple mergers in the ancestry, which will thus only consist of binary mergers. Any other choice of Λ will yield an ancestry with up to four simultaneous multiple mergers at each chromosome, corresponding to the four possible parental chromosomes involved in the forwards-in-time reproduction event, and thus produce ancestries described by a Ξ -coalescent. See [Möhle and Sagitov, 2003, Section 6] for details of Ξ -coalescents arising out of diploid reproduction in this way.

The aim is to show that the ancestry of a sample from the above particle system converges to a structured Ξ -Ancestral Influence Graph [Donnelly and Kurtz, 1999b] as $N \rightarrow \infty$, when time is measured in units of c_N . To establish this fact, we identify the limiting rates of coalescence, mutation, recombination, migration and branching due to selection, and show that these are the only dynamics which affect the ancestry of the process. Throughout, we assume that our sample consists of n_i lineages at deme i , for each $i \in \{1, \dots, D\}$, and that each lineage carries ancestral material on only one chromosome. This assumption is justified later by verifying that a separation of timescales phenomenon [Möhle, 1998] takes place, establishing that distinct chromosomes disperse to separate active lineages instantaneously on the coalescent time scale. For ease of notation, let $n := n_1 + \dots + n_D$ be the total sample size across all demes.

Multiple mergers via a single large family

By the Kingman formula for exchangeable, diploid offspring distributions [Möhle and Sagitov, 2003, equation (9)], the probability of $b \leq n_i$ chromosomes belonging to the same family in the

previous time step with no migration or mutation, recombination or selection taking place is

$$\begin{aligned}
& (1 - \mu_N)^n (1 - r_N)^n \frac{(M_N^{(i)}(t)/2)_{n_i-b+1}}{(M_N^{(i)}(t-1))_{n_i}} \mathbb{E}[(\nu_1^{(i)})_b \nu_2^{(i)} \dots \nu_{n_i-b+1}^{(i)}] \prod_{j \neq i}^D \frac{(M_N^{(j)}(t)/2)_{n_j}}{(M_N^{(j)}(t-1))_{n_j}} \mathbb{E}[\nu_1^{(j)} \dots \nu_{n_j}^{(j)}] \\
& \times \prod_{j=1}^D \left(1 - \sum_{k \neq j}^D m_{jk}^{(N)} \right)^{n_j} \\
& \sim \frac{(2Nd_i)^{1-b}}{2^{n_i-b+1}} \exp\left(\frac{8(b-1)\gamma_i}{d_i \mathbb{E}[(\nu_1)_2]} t\right) \mathbb{E}[(\nu_1^{(i)})_b \nu_2^{(i)} \dots \nu_{n_i-b+1}^{(i)}] \prod_{j \neq i}^D \frac{1}{2^{n_j}} \mathbb{E}[\nu_1^{(j)} \dots \nu_{n_j}^{(j)}].
\end{aligned}$$

Analogously to [Sagitov, 1999, equation (21)], conditions (5), (7), and (8) imply that

$$\frac{(2Nd_i)^{1-b}}{2^{n_i-b+1}} \mathbb{E}[(\nu_1^{(i)})_b \nu_2^{(i)} \dots \nu_{n_i-b+1}^{(i)}] \prod_{j \neq i}^D \frac{1}{2^{n_j}} \mathbb{E}[\nu_1^{(j)} \dots \nu_{n_j}^{(j)}] \sim c_N \frac{4}{d_i} \int_0^1 x^{b-2} (1-x)^{n_i-b} \Lambda(dx),$$

because as in [Sagitov, 1999, equations (4), (5) and (6)], condition (6) implies

$$\prod_{j \neq i}^D \frac{1}{2^{n_j}} \mathbb{E}[\nu_1^{(j)} \dots \nu_{n_j}^{(j)}] \sim \prod_{j \neq i}^D \left(1 - 4c_N \int_0^1 \frac{1 - (1-x)^{n_j} - n_j x (1-x)^{n_j-1}}{x^2} \Lambda(dx) \right) \sim 1.$$

Within families, individuals choose their parent and parental chromosome uniformly at random. Summing over all merger sizes into one common family, and all assignments of offspring into four parental chromosomes, yields the combinatorial expression

$$c_N \frac{4}{d_i} \exp\left(\frac{8(b-1)\gamma_i}{d_i \mathbb{E}[(\nu_1)_2]} t\right) \sum_{l=0}^{(n_i-b) \wedge (4-r)} \binom{n_i-b}{l} \frac{(4)_{r+l}}{4^{b+l}} \int_0^1 x^{b+l-2} (1-x)^{n_i-b-l} \Lambda(dx) \quad (16)$$

for the merger involving $b_1 + \dots + b_r = b \leq n_i$ lineages merging in $r \leq 4$ simultaneous mergers, where each $b_j \geq 2$.

Multiple mergers via two or more large families

The probability of mergers via two or more large families, i.e. families with at least two offspring in the sample, on at least one island is bounded above by the probability of two large families appear simultaneously.

Again by the Kingman formula, this probability is

$$(1 - \mu_N)^n (1 - r_N)^n \frac{(M_N^{(i)}(t)/2)_2}{(M_N^{(i)}(t-1))_4} \mathbb{E}[(\nu_1^{(i)})_2 (\nu_2^{(i)})_2] \sim \frac{1}{16N^2 d_i^2} \mathbb{E}[(\nu_1^{(i)})_2 (\nu_2^{(i)})_2] = o(c_N)$$

by (7).

A single migration event

The event that all n lineages belong to different families in the previous generation, and that

one individual migrates from deme i_1 to i_2 in reverse time, has probability

$$\begin{aligned}
& (1 - \mu_N)^n (1 - r_N)^n \left(1 - \sum_{i=1}^D \frac{M_N^{(i)}(t-1) m_{i_1}^{(N)}}{M_N^{(i_1)}(t-1)} \right)^{n_{i_1}-1} \frac{M_N^{(i_2)}(t-1) m_{i_2 i_1}^{(N)}}{M_N^{(i_1)}(t-1)} \\
& \left[\prod_{i \neq i_1}^D \left(1 - \sum_{j=1}^D \frac{M_N^{(j)}(t-1) m_{ji}^{(N)}}{M_N^{(i)}(t-1)} \right)^{n_i} \right] \left(\prod_{i=1}^D \frac{(M_N^{(i)}(t)/2)^{n_i} \mathbb{E}[\nu_1^{(i)} \dots \nu_{n_i}^{(i)}]}{(M_N^{(i)}(t-1))^{n_i}} \right) \\
& \sim \left(1 - \sum_{i=1}^D m_{i_1 i}^{(N)} \right)^{n_{i_1}-1} n_{i_1} \frac{d_{i_2}}{d_{i_1}} \exp \left(\frac{8t}{\mathbb{E}[(\nu_1)_2]} \left[\frac{\gamma_{i_1}}{d_{i_1}} - \frac{\gamma_{i_2}}{d_{i_2}} \right] \right) m_{i_2 i_1}^{(N)} \left[\prod_{i \neq i_1}^D \left(1 - \sum_{j=1}^D m_{ij}^{(N)} \right)^{n_i} \right] \\
& \sim c_N n_{i_1} \frac{d_{i_2}}{d_{i_1}} \exp \left(\frac{8t}{\mathbb{E}[(\nu_1)_2]} \left[\frac{\gamma_{i_1}}{d_{i_1}} - \frac{\gamma_{i_2}}{d_{i_2}} \right] \right) m_{i_2 i_1},
\end{aligned}$$

by (4) and (11). In order to obtain a time-homogeneous migration rate parameter, which is not necessary but which we assume for simplicity, we take $\gamma_i/d_i \equiv \gamma_j/d_j$ for all pairs of demes $i, j \in \{1, \dots, D\}$, leading to the migration rate

$$c_N n_{i_1} \frac{d_{i_2}}{d_{i_1}} m_{i_2 i_1} =: c_N n_{i_1} \tilde{m}_{i_1 i_2}.$$

A similar calculation demonstrates that the analogous probability for more than one migration event is $o(c_N)$, while combining the above with the first two calculations demonstrates that a single migration occurring simultaneously with one or more large families is also an $o(c_N)$ event.

A single mutation event

An analogous calculation to the migration case using (9) shows that the probability of one site mutating in the previous time step with no other accompanying events converges to $c_N n \theta$, and that multiple simultaneous mutations are an event of $o(c_N)$ probability and hence vanish in the limit as $N \rightarrow \infty$.

A single recombination event

Likewise, an analogous calculation to the migration case using (10) shows that the probability of one chromosome recombining in the previous time step with no other accompanying events converges to $c_N n \rho$, and that multiple simultaneous recombinations have probability $o(c_N)$ and hence vanish in the $N \rightarrow \infty$ limit.

A single branching event due to a selective birth

The probability of a lineage belonging to a selective birth by a family in the previous generation depends on the fitness of its parents, which is unknown. An elegant solution, dating back to [Krone and Neuhauser, 1997] is to simulate selective events at the greatest possible rate $s_N^* := \max\{s_N(\cdot, \cdot)\}$, add the $4L$ chromosomes belonging to the two potential parents into the sample along with retaining the child lineage whenever a selection event happens, and track this extended sample to its *ultimate ancestor*: the most recent common ancestor of the original sample, as well as all potential selective parents encountered along the way. The type of the ultimate ancestor can then be sampled from the stationary distribution of M (or any other desired initial law), with mutations occurring along lineages and alleles propagated to children as before. Now the alleles, and thus the fitness of the selective parents are known at each potential selective event, and the true ancestry of each child lineage can be assigned to either a randomly chosen parent with probability s_N/s_N^* , or to remain with the ongoing child lineage with probability $1 - s_N/s_N^*$.

From the point of view of the ancestral process, such selective branching events in which one lineage branches into $4L + 1$ lineages (corresponding to the single-chromosome child lineage, as

well as the $4L$ parental chromosomes which immediately disperse into separate lineages due to separation of time scales) happens with probability

$$(1 - \mu_N)^n (1 - r_N)^n \prod_{i=1}^D \left\{ \left(1 - \sum_{j \neq i}^D m_{ij}^{(N)} \right)^{n_i} \frac{(M_N^{(i)}(t))_{n_i}}{(M_N^{(i)}(t-1))_{n_i}} \mathbb{E}[\nu_1^{(i)} \dots \nu_{n_i}^{(i)}] \right\} n s_N^* \sim c_N n \sigma^*$$

by (12), (13), and (15).

Dispersal of chromosomes into distinct, single-marked individuals

Finally, we abandon the assumption all lineages carrying ancestral material on only one chromosome in order to verify the separation of time scales phenomenon.

The probability of $n/2$ double-marked individuals with tracked material on each chromosome on each pair dispersing into single-marked parents, each of whom carries ancestral material on only one chromosome in each pair, in the previous generation is $O(1)$, because every individual is replaced at every time step, and individuals always inherit one chromosome from each parent. Thus, complete dispersal of $n/2$ double-marked individuals happens in one generation provided that all $n/2$ individuals originate from different families. This happens with probability

$$\prod_{i=1}^D \frac{(M_N^{(i)}(t))_{n_i}}{(M_N^{(i)}(t-1))_{n_i}} \mathbb{E}[\nu_1^{(i)} \dots \nu_{n_i}^{(i)}] \sim 1.$$

Likewise, the probability of two active chromosomes belonging to distinct pairs splitting apart into distinct ancestors is $1/2 = O(1)$ because assignments of parents to chromosomes is done independently and uniformly at random. Hence, the probability of a lineage with $2L$ ancestral chromosomes dispersing into $2L$ lineages with a single ancestral chromosome each in at most $2L - 1$ generations happens with probability at least

$$\left(\frac{1}{2}\right)^{2L} \prod_{t=1}^{2L} \prod_{i=1}^D \frac{(M_N^{(i)}(t))_{n_i}}{(M_N^{(i)}(t-1))_{n_i}} \mathbb{E}[\nu_1^{(i)}(t) \dots \nu_{n_i}^{(i)}(t)] = O(1).$$

Probabilities of merger, recombination, selection or migration events were all established above to be $O(c_N)$, and thus the probability of single dispersal event before any merger, recombination, selection or migration events has probability of order

$$\frac{1}{1 + A c_N} \rightarrow 1,$$

where $A > 0$ is a constant independent of both n and N . Thus an analogue of the separation of timescales result in [Möhle, 1998] holds, which justifies considering only single-marked configurations in the previous computations of transition probabilities.

Remark 2. The above calculations have been presented with the exponential population growth model defined in (3) for concreteness, but this choice is not essential. For instance, the algebraic population growth model

$$M_N^{(i)} := 2 \left[N d_i \left(1 + \frac{t}{2 \lfloor N d_i \rfloor} \right)^{-\gamma_i} \right]$$

yields the same rates of mutation, branching due to recombination, and branching due to weak selection. The rate of multiple mergers via a single large family becomes

$$c_N \frac{4}{d_i} \left(1 + \frac{8t}{d_i \mathbb{E}[(\nu_1)_2]} \right)^{\gamma_i(b-1)} \sum_{l=0}^{(n_i-b) \wedge (4-r)} \binom{n_i-b}{l} \frac{(4)_{r+l}}{4^{b+l}} \int_0^1 x^{b+l-2} (1-x)^{n_i-b-l} \Lambda(dx),$$

and the migration rate from deme i_1 to i_2 in reverse time becomes

$$c_N n_{i_1} \frac{d_{i_2} \left(1 + \frac{8t}{d_{i_1} \mathbb{E}[(\nu_1)_2]}\right)^{\gamma_{i_1}}}{d_{i_1} \left(1 + \frac{8t}{d_{i_2} \mathbb{E}[(\nu_1)_2]}\right)^{\gamma_{i_2}}} m_{i_2 i_1}.$$

In this case it will be necessary to take both $\gamma_i \equiv \gamma_j$ and $d_i \equiv d_j$ for all pairs of demes $i, j \in \{1, \dots, D\}$ in order to obtain the simpler, time-independent reverse time rate of migration

$$c_N n_{i_1} \frac{d_{i_2}}{d_{i_1}} m_{i_2 i_1} =: c_N n_{i_1} \tilde{m}_{i_1 i_2}.$$

4 Robustness results

The following three subsections quantify the respective effect of selection, recombination, and population structure on the sampling distribution of the singleton-tail statistic. Each subsection specialises the model of Section 3 to consist of only the relevant evolutionary force by a particular choice of parameters. We assume the model of Schweinsberg [2003] for the evolution of the population, and thus consider a one-dimensional family of processes specified by $\Lambda(dy) = \text{Beta}(2 - \alpha, \alpha)(dy)$ in (8) for $\alpha \in (1, 2]$, with corresponding time scalings $c_N \sim N^{1-\alpha}$.

It will also be necessary to distinguish between two kinds of data sets: simulated data used to fit approximate likelihoods and calibrate the hypothesis test, as well as observed data, which will also be simulated in this instance, but which will typically be a biological data set. We will refer to the former as calibration data, and the latter as observed data. A C++ implementation of the algorithm used to generate the data in this section is available at <https://github.com/JereKoskela/Beta-Xi-Sim>.

For all subsequent simulations, we set the number of replicates per model to 1000, the sample size to $n = 500$, the lumped tail cutoff to $k = 15$, and assume the true mutation rate is known. The number of unlinked chromosomes per sample is set to 23 to match the number of linkage groups in Atlantic cod [Tørresen et al., 2017, Supplementary Table 3] — an organism for which multiple merger have frequently been suggested as an important evolutionary mechanism [Steinrücken et al., 2013, Tellier and Lemaire, 2014]. Results are averaged across chromosomes as outlined in Section 2. The physical lengths of the 23 chromosomes have also been set to match those reported in [Tørresen et al., 2017, Supplementary Table 3]. The approximate size of hypothesis tests is set at $\omega = 0.01$ throughout.

4.1 Weak selection

In this section we consider the model of Section 3 with a single deme ($D = 1$), no migration ($m_{ij} \equiv 0$) and no recombination ($\rho = 0$). The resulting process is a Ξ -coalescent analogue of the Complex Selection Graph of Fearnhead [2003]. We compute realisations of the singleton-tail statistic by assuming that neutral, infinitely-many-sites mutations occur on each chromosome along the branches of the realised non-neutral tree sampled from the Ξ -CSG, but that the selective types of individuals are unobserved. This assumption is reasonable if the selective advantage of individuals cannot be observed directly, and if mutations with a selective advantage are either much less frequent than neutral mutations, or occur in an unobserved region of each chromosome.

Figure 1 shows four comparisons of sampling distributions between neutral and non-neutral models. The fitness model assumes two alleles, a and A , with each chromosome pair contributing fitness σ if either parent carries at least one A allele at that pair, and 0 otherwise. The

selection rates are necessarily low, because the cost of simulating the ASGs is known to increase exponentially in σ [Fearnhead, 2001, Appendix A]. Efficiency gains resulting from perfect simulation techniques [Fearnhead, 2001, 2003] cannot be employed here because they rely on terminating the simulation before reaching the MRCA, and thus a full SFS cannot be resolved.

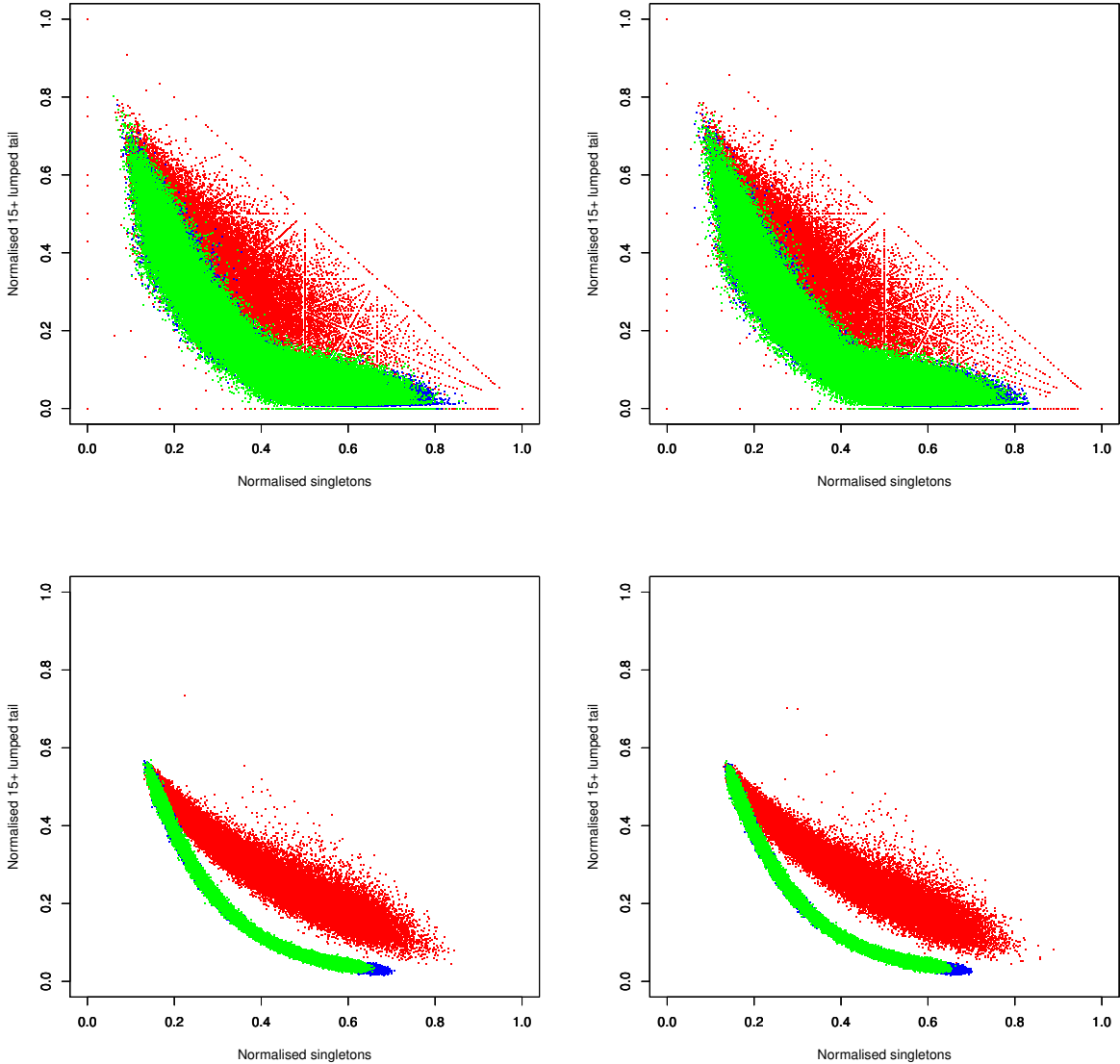


Figure 1: Scatter plots of realisations of the singleton-tail statistic for each model in Θ_0 and Θ_1 . Realisations of Ξ -coalescents are in red, exponential growth models in blue, and algebraic growth models in green. (Top Row) Each sample consists of one chromosome, and $\sigma = 0$ (Left) or $\sigma \in (0.0045, 2.25)$ as α varies from 1 to 2 (Right). (Bottom Row) Each sample consists of 23 chromosomes, and $\sigma = 0$ (Left) or $\sigma \in (0.000004, 0.002)$ as α varies from 1 to 2 (Right).

Both the single chromosome and the 23 chromosome results in Figure 1 show striking agreement between sampling distributions in the neutral and selective cases. In the 23 chromosome case this might be attributed to the very low selection rate, though the resulting ancestral graphs did still contain appreciable numbers of branching events, but the single chromosome simulation rules out this simple explanation. Instead, these simulations provide strong evidence that the distribution of relative branch lengths from realised tree drawn from an Ancestral Selection Graph closely resembles that of a neutral tree simulated directly, at least for external branches,

and the oldest branches before the MRCA is reached. Thus, the distributions of neutral SFs simulated along these trees will also be very similar, meaning that the singleton-tail statistic cannot be used to detect weak selection, but can be used to discriminate between population growth and multiple merger models without knowing whether weak selection is taking place.

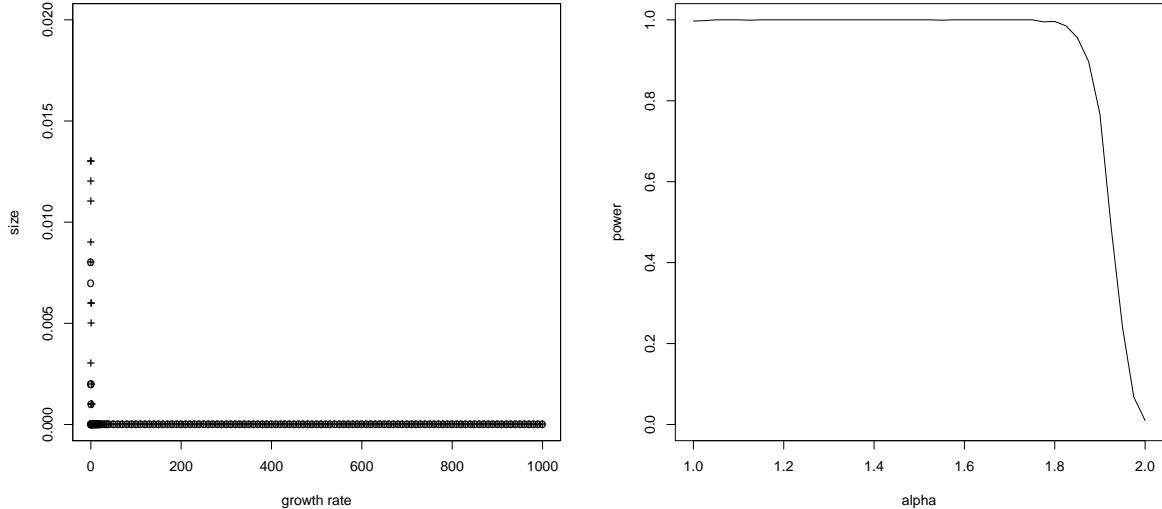


Figure 2: Empirical size (left) and power (right) of a Θ_0 vs Θ_1 test conducted using calibration data simulated under neutral models, but applied to observed data simulated from selective models. On the left, sizes under algebraic growth models are denoted by circles, while sizes under exponential growth models are denoted by pluses, though the two profiles are indistinguishable. The simulation parameters are as in the bottom row of Figure 1.

Figure 2 confirms that the presence or absence of selection is insignificant, by conducting the hypothesis test (1) by computing approximate sampling distributions and a rejection region using calibration data from neutral models, and applying the resulting misspecified test to observed data simulated from coalescent models including weak selection. Both the size and power of the test are unaffected by the misspecification of the model.

4.2 Recombination

In this section we consider the model of Section 3 with a single deme ($D = 1$), no migration ($m_{ij} \equiv 0$) and no selection ($\sigma^* = 0$). As in the previous section, realisations of the singleton-tail statistic are computed by assuming a neutral, infinitely-many-sites mutation model along the branches of the realised Ξ -Ancestral Recombination Graph.

Figure 3 presents a comparison between models with and without recombination. As was the case with weak selection (see Figure 1), the presence of recombination makes no discernible difference to the sampling distribution of the singleton-tail statistic. Figure 4 demonstrates that the size and power of statistical tests are unaffected when a misspecified model which incorrectly neglects recombination is used to generate calibration data, and the hypothesis test is conducted on observed data with recombination.

4.3 Population structure

In this section we consider the model of Section 3 with a no selection ($\sigma^* = 0$), no recombination ($\rho = 0$), and several different patterns of population structure.

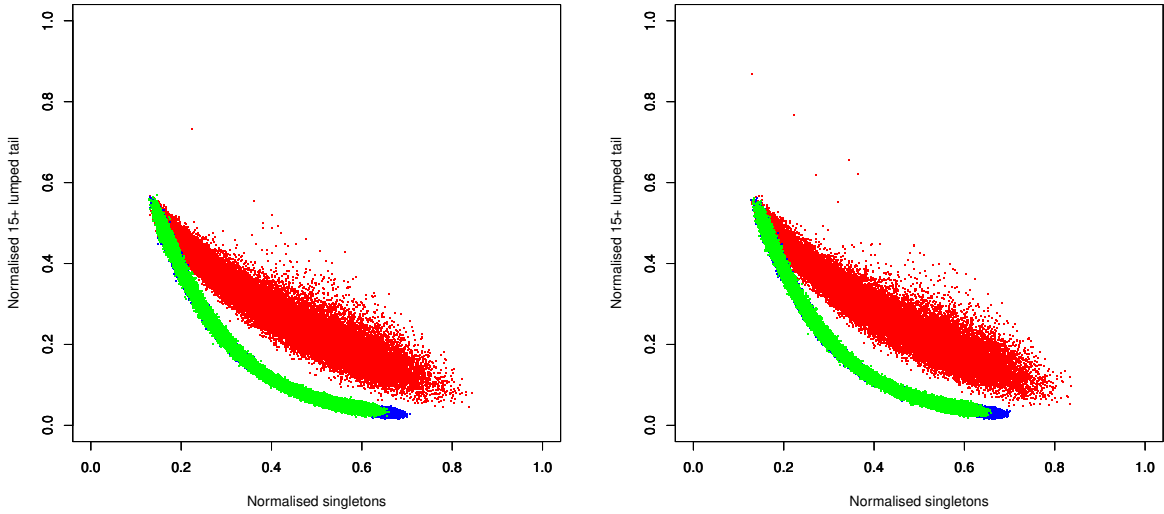


Figure 3: Scatter plots of 1000 realisations of the singleton-tail statistic for each model in Θ_0 and Θ_1 . Realisations of Ξ -coalescents are in red, exponential growth models in blue, and algebraic growth models in green. (Left) $\rho = 0$. (Right) $\rho \in (0.001, 0.5)$ as α varies from 1 to 2.

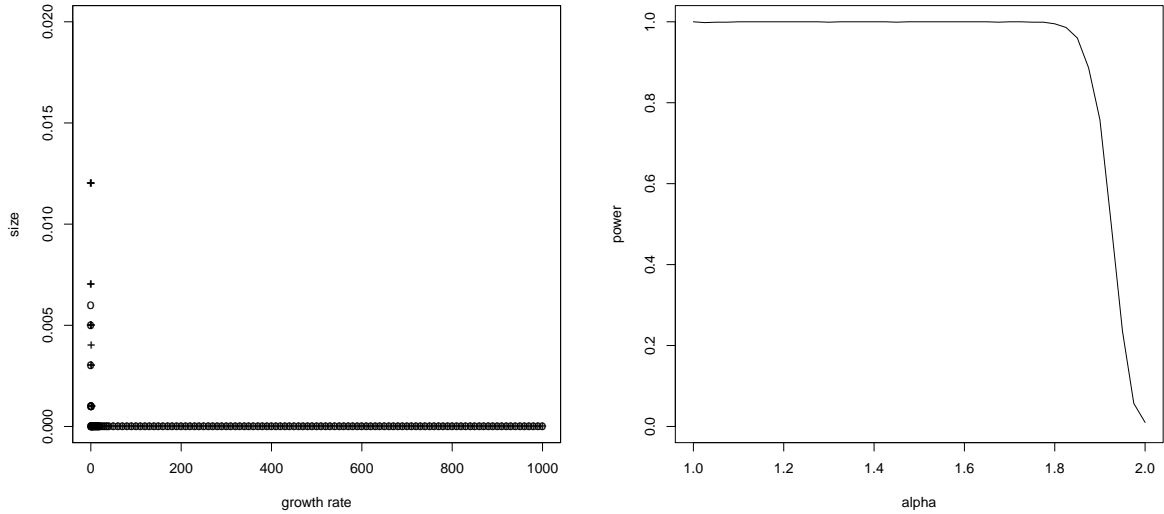


Figure 4: Empirical size (left) and power (right) of a Θ_0 vs Θ_1 test conducted using calibration data simulated under models without recombination, but applied to observed data simulated under models with recombination. On the left, sizes under algebraic growth models are denoted by circles, while sizes under exponential growth models are denoted by pluses, though the two profiles are indistinguishable. The simulation parameters are as in Figure 3.

Figure 5 shows sampling distributions corresponding to a four deme model with symmetric migration between all pairs of demes, as well as a two deme model with asymmetric migration. In contrast to earlier sections on weak selection and recombination, these scatter plots differ markedly from the panmictic results in Figures 1 and 3, and also from each other. Figure 6 demonstrates that either neglecting or misspecifying spatial structure results in very poor performance of the hypothesis test. The false positive rate does not remain below the specified size, and the power is indistinguishable from zero across the majority of the parameter range.

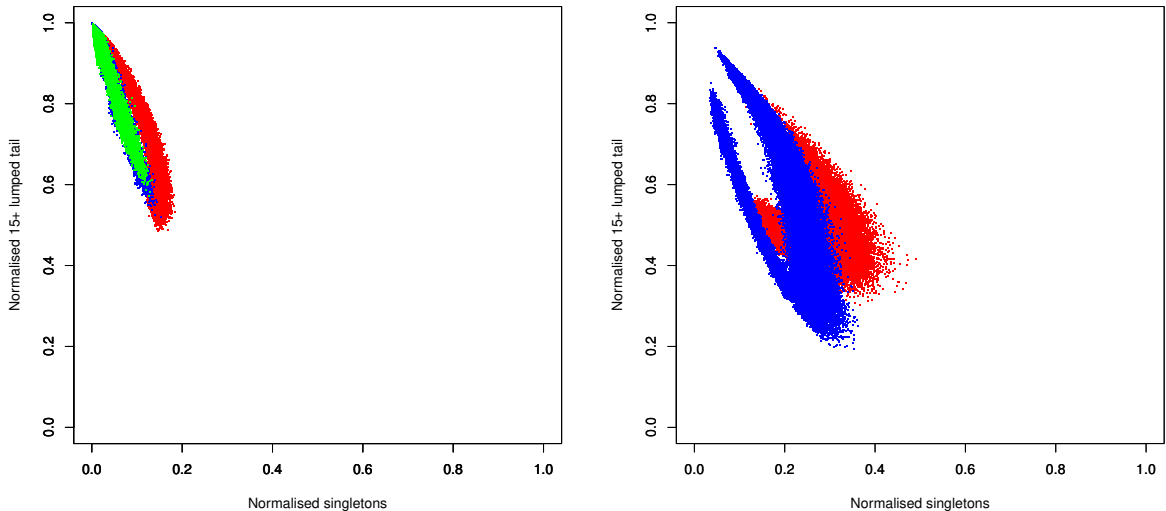


Figure 5: Scatter plots of realisations of the singleton-tail statistic for each model in Θ_0 and Θ_1 . Realisations of Ξ -coalescents are in red, exponential growth models in blue, and algebraic growth models in green. (Left) Four demes with equal population sizes and symmetric migration between all pairs of demes at reverse-time rate $\tilde{m} \in (0.01, 5)$ as α varies from 1 to 2. (Right) Two demes with relative population sizes $(0.75, 0.25)$, and reverse-time migration rate ranging from $(\tilde{m}_{12}, \tilde{m}_{21}) = (0.01/3, 0.03)$ when $\alpha = 1$ to $(\tilde{m}_{12}, \tilde{m}_{21}) = (5/3, 15)$ when $\alpha = 2$. The green point cloud is absent because our null model requires symmetric mutation under algebraic growth, but not under Ξ -coalescents or exponential growth. The null hypothesis Θ_0 also contains five additional points $\gamma \in \{0.0125, 0.025, 0.05, 0.075, 0.15\}$ in order to ensure smooth coverage of the range of realisations.

5 Distinguishing high fecundity from selective sweeps

In this section we focus on distinguishing between multiple mergers due to selective sweeps and multiple mergers due to high fecundity. Specifically, we assume that mutations providing a strong selective advantage occur at random, and sweep to fixation on a time scale that is fast enough to both cause multiple mergers in the ancestral model, and to disallow multiple concurrent sweeps. However, genetic material which is unlinked to the beneficial mutation escapes the selective sweep, and thus a multiple merger only affects one chromosome at a time. We also assume that recombination within chromosomes results in incomplete sweeps, so that when viewed backwards in time each individual has a random chance to participate in the merger resulting from each sweep. We choose these random participation probabilities to be drawn from a $\text{Beta}(2-\alpha, \alpha)$ -distribution, so that when the population is diploid and biparental, the resulting marginal coalescent at each chromosome is the Ξ -coalescent with merger rates given by (16).

Remark 3. The model described above closely resembles a Λ -coalescent model by Durrett and Schweinsberg [2005], in which multiple mergers were also caused by the joint effect of selective sweeps and recombination. However, their convergence result can only be used to obtain Λ -coalescents in which Λ has an atom at 0, and hence it does not strictly apply here [Durrett and Schweinsberg, 2005, Example 2.5]. A model akin to the one described above could be constructed similarly by letting selective sweeps occur more frequently than the time scale of pairwise coalescence, thus causing the atom at 0 to vanish in the large population limit [Gillespie, 2000, Durrett and Schweinsberg, 2005].

We fix our null hypothesis as the class of selective sweep models described above with the

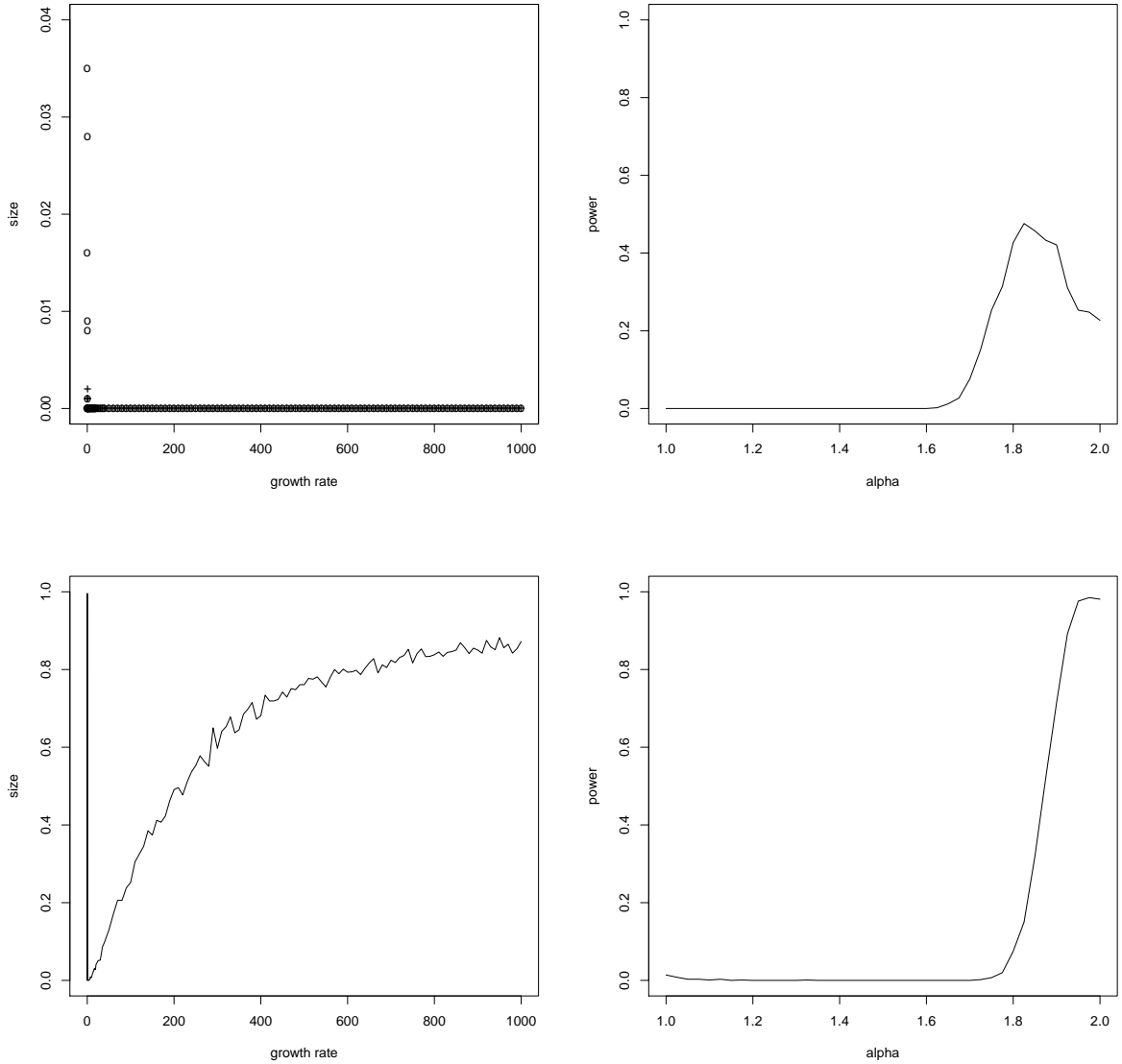


Figure 6: (Top Row) Empirical size (Left) and power (Right) of a test of Θ_0 vs Θ_1 conducted using calibration data simulated under panmictic models, but applied to observed data simulated under the four deme model. On the left, sizes under algebraic growth models are denoted by circles, while sizes under exponential growth models are denoted by pluses, though the two profiles are indistinguishable (Bottom Row) Empirical size (Left) and power (Right) of a test of Θ_0 vs Θ_1 conducted using calibration data simulated under the four deme model, but applied to observed data simulated under the two deme model. The size profile on the left is for exponential growth only since algebraic population growth is excluded in the asymmetric migration setting. The simulation parameters in both cases are as in Figure 5.

parameter $\alpha \in (1, 2)$ discretised as in (2). The alternative hypothesis is the model of Section 3 with a single deme, $D = 1$, as well as no selection, recombination or migration: $\sigma^* = \rho = m_{ij} = 0$. Thus, the only difference between the two model classes is whether coalescence times at unlinked chromosomes are independent, or positively correlated. The marginal processes at each chromosome coincide.

Figure 7 demonstrates that the singleton-tail statistic exhibits higher sampling variance under the alternative hypothesis than under the null, as expected due to positive correlation between

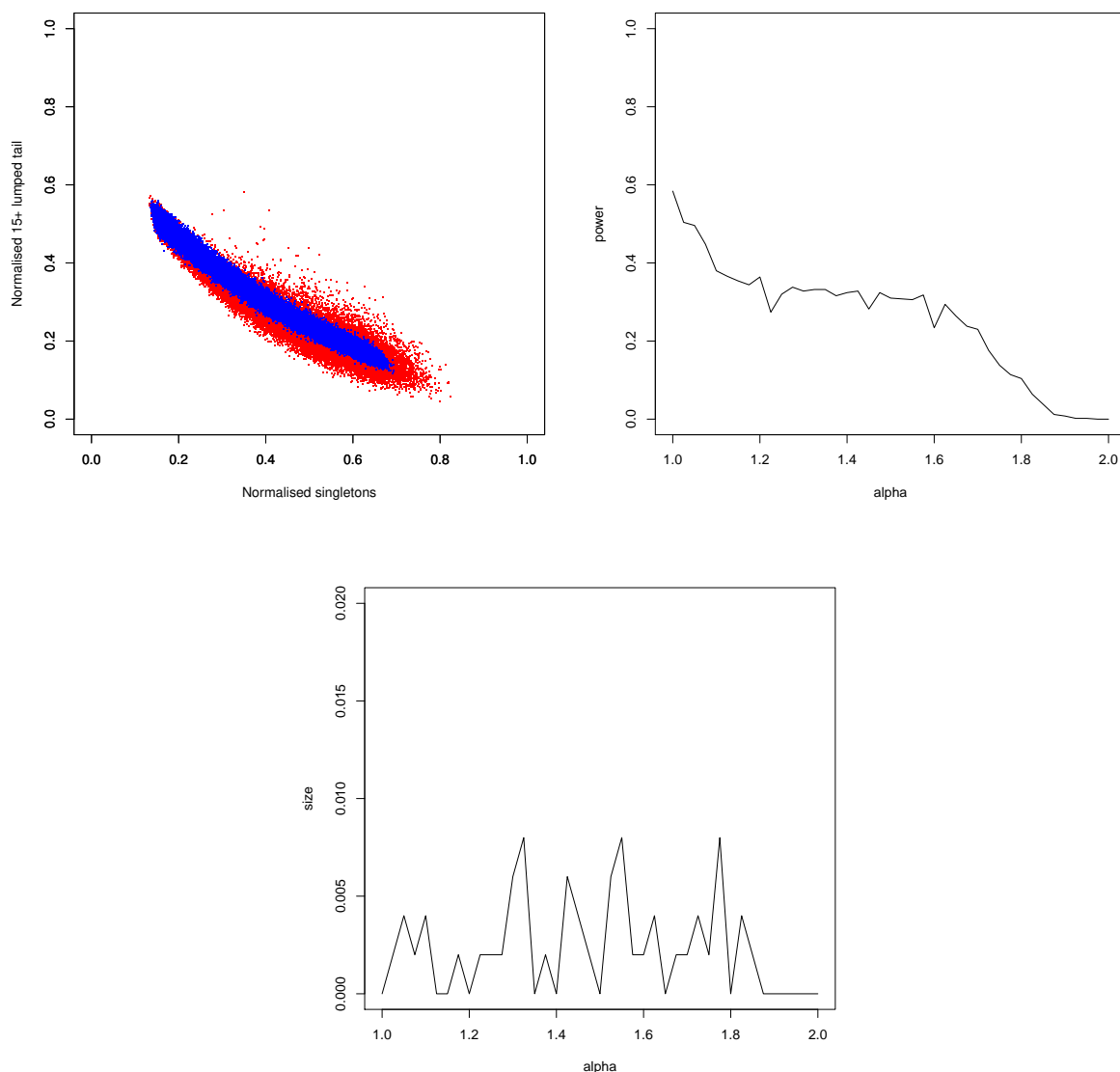


Figure 7: (Top Left) Sampling distribution of the singleton-tail statistic under the null hypothesis in blue, and the alternative hypothesis in red. (Top Right) Empirical power of the likelihood ratio test (1). (Bottom) Empirical size of the likelihood ratio test (1).

chromosomes. While the sampling distributions under both hypotheses centre on the same mean, increased variance means that the null hypothesis can be correctly rejected with moderate power above 30% for the majority of the parameter range. Reversing the roles of the hypotheses would cause the power to vanish, as then the bulk of the sampling distribution under the alternative (selective sweep) hypothesis would be fully contained in that of the null (high fecundity) hypothesis.

In contrast to Section 4, the calibration data set and the observed data set used to obtain empirical sizes in Figure 7 coincide. As a consequence, the data sets in this section were split into two equal halves, one of which was used to fit the KDEs and estimate the quantile q_ω , while the other was used to obtain empirical powers and sizes. Hence, estimates in Figure 7 are based on 500 realisations, not 1000 as in Section 4.

6 Discussion

We have derived coalescent models of population growth and high fecundity in complex biological scenarios involving multiple chromosomes under the joint effect of weak natural selection, crossover recombination, and spatial population structure. We then studied the effect of these three confounders on the ability of the singleton-tail statistic Koskela [2018] to distinguish between population growth models and Ξ -coalescent models involving multiple mergers arising from high fecundity reproduction.

Both crossover recombination and weak natural selection were found to have no effect on the sampling distribution of the singleton-tail statistic, and hence the singleton-tail statistic retains its ability to distinguish these two models from multi-chromosome data with very high power. Moreover, model selection can be conducted based on calibration data simulated from a neutral model without recombination. In addition to a reduction in the dimension of the parameter space, this yields significant efficiency gains because selection and recombination both carry a heavy computational burden, which can thus be avoided.

In contrast, population structure has a significant effect on the sampling distribution of the singleton-tail statistic. Neglecting or misspecifying population structure was found to dramatically reduce the statistical power of hypothesis tests conducted based on the singleton-tail statistic, and also elevate the false positive rate above the specified test size in some cases. This finding motivates further research into methods which can infer population structure from data without assuming a particular population growth scenario or Ξ -coalescent model.

Finally, we investigated the ability of the singleton-tail statistic to distinguish between multiple mergers arising due to selective sweeps, and multiple mergers arising due to high fecundity. This is a challenging model selection problem because the marginal models at individual chromosomes coincide under the two hypotheses. However, ancestral trees at unlinked chromosomes are independent under the null hypothesis, and positively correlated under the alternative hypothesis. The resulting increase in sampling variance of the singleton-tail statistic enabled us to distinguish a high fecundity alternative hypothesis from a selective sweep null hypothesis with moderate power. Reversing the roles of the hypotheses would cause the power of the test to vanish, and thus model selection can only be successfully performed in one direction based on this method.

Acknowledgements

The authors are grateful to Jochen Blath and Bjarki Eldon for discussions concerning generalised Beta- Ξ -coalescent models. JK was supported by Deutsche Forschungsgemeinschaft (DFG) grant BL 1105/3-2 as part of SPP Priority Programme 1590. MWB was supported by DFG grant BL 1105/5-1 as part of SPP Priority Programme 1590. Both authors were also supported by DFG SPP Priority Programme 1819 start-up module grant “Population genomics of highly fecund codfish”.

References

- E Árnason. Mitochondrial cytochrome *b* variation in the high-fecundity Atlantic cod: trans-Atlantic clines and shallow gene genealogy. *Genetics*, 166:1871–1885, 2004.
- A T Beckenbach. Mitochondrial haplotype frequencies in oysters: neutral alternatives to selection models. In B Golding, editor, *Non-Neutral Evolution*, pages 188–198. Chapman & Hall, New York, 1994.

- M Birkner, J Blath, and M Steinrücken. Importance sampling for Lambda-coalescents in the infinitely many sites model. *Theor Pop Biol*, 79:155–173, 2011.
- M Birkner, J Blath, and B Eldon. An ancestral recombination graph for diploid populations with skewed offspring distribution. *Genetics*, 193:255–290, 2013.
- P Donnelly and T G Kurtz. Particle representations for measure-valued population models. *Ann Probab*, 27:166–205, 1999a.
- P Donnelly and T G Kurtz. Genealogical processes for Fleming-Viot models with selection and recombination. *Ann Appl Probab*, 9:1091–1148, 1999b.
- R Durrett and J Schweinsberg. A coalescent model for the effect of advantageous mutations on the genealogy of a population. *Stoch Proc Appl*, 115:1628–1657, 2005.
- B Eldon. Structured coalescent processes from a modified Moran model with large offspring numbers. *Theor Pop Biol*, 76:92–104, 2009.
- B Eldon and J Wakeley. Coalescent processes when the distribution of offspring number among individuals is highly skewed. *Genetics*, 172:2621–2633, 2006.
- B Eldon, M Birkner, J Blath, and F Freund. Can the site frequency spectrum distinguish exponential population growth from multiple-merger coalescents. *Genetics*, 199(3):841–856, 2015.
- P Fearnhead. Perfect simulation from population genetic models with selection. *Theor Pop Biol*, 59:263–279, 2001.
- P Fearnhead. Ancestral process for non-neutral models of complex diseases. *Theor Pop Biol*, 63:115–130, 2003.
- Y X Fu. Statistical properties of segregating sites. *Theor Pop Biol*, 48:172–197, 1995.
- J H Gillespie. Genetic drift in an infinite population: the pseudohitchhiking model. *Genetics*, 155:909–919, 2000.
- R C Griffiths and P Marjoram. An ancestral recombination graph. In P Donnelly and S Tavaré, editors, *Progress in population genetics and human evolution*, pages 257–270. Springer Verlag, Berlin, 1997.
- D Hedgecock and A I Pudovkin. Sweepstakes reproductive success in highly fecund marine fish and shellfish: a review and commentary. *Bull Mar Sci*, 87:971–1002, 2011.
- H M Herbots. The structured coalescent. In P Donnelly and S Tavaré, editors, *Progress in population genetics*, pages 231–255. Springer, New York, 1997.
- R R Hudson. Properties of a neutral allele model with intragenic recombination. *Theor Pop Biol*, 23:183–201, 1983a.
- R R Hudson. Testing the constant-rate neutral allele model with protein sequence data. *Evolution*, 37:203–217, 1983b.
- J F C Kingman. The coalescent. *Stoch Proc Appl*, 13:235–248, 1982a.
- J F C Kingman. Exchangeability and the evolution of large populations. In G Koch and F Spizzichino, editors, *Exchangeability in probability and statistics*, pages 97–112. North-Holland, Amsterdam, 1982b.
- J F C Kingman. On the genealogy of large populations. *J Appl Probab*, 19A:27–43, 1982c.
- J Koskela. Multi-locus data distinguishes between population growth and multiple merger coalescents. *Stat Appl Genet Mol Biol*, 17(3):20170011, 2018.

- S M Krone and C Neuhauser. Ancestral processes with selection. *Theor Pop Biol*, 51:210–237, 1997.
- M Möhle. A convergence theorem for Markov chains arising in population genetics and the coalescent with selfing. *Adv in Appl Probab*, 30:493–512, 1998.
- M Möhle and S Sagitov. Classification of coalescent processes for haploid exchangeable coalescent processes. *Ann Probab*, 29:1547–1562, 2001.
- M Möhle and S Sagitov. Coalescent patterns in diploid exchangeable population models. *J Math Biol*, 47:337–352, 2003.
- C Neuhauser and S M Krone. The genealogy of samples in models with selection. *Genetics*, 145:519–534, 1997.
- J Pitman. Coalescents with multiple collisions. *Ann Probab*, 27:1870–1902, 1999.
- S Sagitov. The general coalescent with asynchronous mergers of ancestral lines. *J Appl Probab*, 36:1116–1125, 1999.
- O Sargsyan and J Wakeley. A coalescent process with simultaneous multiple mergers for approximating the gene genealogies of many marine organisms. *Theor Pop Biol*, 74:104–114, 2008.
- J Schweinsberg. Coalescents with simultaneous multiple collisions. *Electron J Probab*, 5:1–50, 2000.
- J Schweinsberg. Coalescent processes obtained from supercritical Galton-Watson processes. *Stoch Proc Appl*, 106:107–139, 2003.
- M Steinrücken, M Birkner, and J Blath. Analysis of DNA sequence variation within marine species using beta-coalescents. *Theor Pop Biol*, 87:15–24, 2013.
- F Tajima. Evolutionary relationship of DNA sequences in finite populations. *Genetics*, 105:437–460, 1983.
- A Tellier and C Lemaire. Coalescence 2.0: a multiple branching of recent theoretical developments and their applications. *Mol Ecol*, 23:2637–2652, 2014.
- O K Tørresen, B Star, S Jentoft, W B Reinart, H Grove, J R Miller, B P Walenz, J Knight, J M Ekholm, P Peluso, R B Edvardsen, A Tooming-Klunderud, M Skage, S Lien, K S Jakobsen, and A J Nederbragt. An improved genome assembly uncovers prolific tandem repeats in Atlantic cod. *BMC Genomics*, 18(1):95, 2017.
- G A Watterson. On the number of segregating sites in genetical models without recombination. *Theor Pop Biol*, 7:1539–1546, 1975.